Contents list available at CBIORE journal website

International Journal of Renewable Energy Development

Journal homepage: https://ijred.cbiore.id

Research Article

Production of biodiesel by using CaO nano-catalyst synthesis from mango leaves extraction

Sarah Shakir Mahmood* and Atheer Mohammed Al-Yaqoobi

Department of Chemical Engineering, College of Engineering, University of Baghdad, Iraq

Abstract. Development and population expansion have the lion's share of driving up the fuel cost. Biodiesel has considerable attention as a renewable, ecologically friendly and alternative fuel source. In this study, CaO nanocatalyst is produced from mango leaves as a catalysis for the transesterification of waste cooking oil (WCO) to biodiesel. The mango tree is a perennial plant, and its fruit holds significant economic worth due to its abundance of vitamins and minerals. This plant has a wide geographical range and its leaves can be utilized without any negative impact on its growth and yield. An analysis was conducted to determine the calcium content in the fallen leaves, revealing a significant quantity of calcium that holds potential for utilization. The catalyst was characterized by different analytic techniques such as XRD, SEM-EDS, FT-IR, and BET analyses. Several parameters impacted on the transesterification process were exploited by conventional transesterification (batch). The result revealed that the optimum reaction was reached at a methanol to oil ratio of 50% w/w, catalyst loading of 3%, temperature of 65°C and reaction time of 1.5 h with a yield of 93.21%, and the activation energy of the transesterification reaction was found to be 38.906 KJ mol^{-1}. The reaction was verified to be irreversible pseudo-first order based on a linear Arrhenius plot and a high R2 value. The catalyst shows good stability and catalytic activity when it is reused and the yield was found to be 80.293% in the 5th cycle.

Keywords: Biodiesel, waste cooking oil (WCO), CaO nanocatalyst, kinetic, heterogenous catalyst, mango leaves.

Received: 17th June 2024; Revised: 26th August2024; Accepted: 17th Sept 2024; Available online: 21th September 2024

1. Introduction

In recent years, fossil resources have become greatly depleted due to increasing population growth and the increasing industrial revolution. Therefore, to reduce environmental pollution resulting from the excessive use of fossil fuel sources and to confront the growing energy crisis, an alternative source of energy that is renewable, sustainable and environmentally friendly has been sough (Al-Yaqoobi, Al-Rikabey and Al-Mashhadani, 2021; Changmai *et al.*, 2021; Abd and AL-yaqoobi, 2024).

Extensive research has been conducted over the past years to develop sustainable and renewable energy such as solar energy (Maka and Alabid, 2022), tidal energy (Masood Ahmad, Kumar and Ranjan, 2022), geothermal (Igwe, 2021), biofuels (Ali Abbas and M. Flayeh, 2019; Abd and Al-Yaqoobi, 2023; Abd, Al-yaqoobi and Abdul-Majeed, 2024), etc. Biodiesel is widely used as an alternative to fossil fuels to enhance combustion efficiency and reduce the release of automobile oxides and sulphur. Biodiesel is extracted from renewable sources and is directly biodegradable (Sahu *et al.*, 2023). It can be used in automobile engines without any change or harm to the engine and it reduces the emissions of CO2 (Hussien and Abdul hameed, 2019). Biodiesel can be defined as a biofuel which consists of fatty acid of a long chain of mono-alkyl ester (Alshahidy and Abbas, 2020; Jurmot and Abbas, 2022). Transesterification and esterification reactions are used to synthesize biodiesel. These reactions include the reactions of various oily raw materials with alcohol and a homogeneous or heterogeneous catalyst present. These reactions are reversible the forward reaction produces biodiesel and glycerol, and the reverse reaction produces saponification reactions (Sahu *et al.*, 2023).

The traditional feedstocks used to produce biodiesel in the transesterification process are edible oils such as rapeseed, sunflower, soybean etc. Utilizing these oils in the production of biodiesel intersects the food chain and causes its price to rise. On the other hand, waste cooking oil (WCO) and non-edible oils such as jatropha, rubber seed oil, and pinata are likely to be suitable alternative feedstock to be used to produce biodiesel (Abdul-Kader *et al.*, 2023).

Homogenous catalysts are classified into base catalysts such as KOH, NaOH, and acid catalysts such as H_2SO_4 which are widely used in the transesterification reaction and show good catalytic activity, resulting in a higher yield through less reaction time, as well they are cheap and available. However, this type of catalyst is escorted by some drawbacks such as the formation of water as by by-product which reduce the yield of biodiesel. Also, homogeneous catalysts require large amounts of water to separate them from the product which increases the cost of the production and contaminates the water (Hadiyanto *et al* 2016). Furthermore, homogeneous catalysts can't be used in the transesterification process when the FFA content is less than 2 wt.% (Changmai *et al.*, 2020).

Meanwhile, heterogeneous catalysts such as MgO, SrO,

* Corresponding author
Email: sarah.s.mohmood@coeng.uobaghdad.edu.iq (S.S.Mahmood)

https://doi.org/10.61435/ijred.2024.60469
ISSN: 2252-4940/© 2024.The Author(s). Published by CBIORE

CaO, and Zeolites are beneficial alternatives to homogeneous catalysts. Where these types of catalysts can be recycled and can separate easily from the product, so they do not need large quantities of water to neutralise and separate from the product besides they produce low byproducts (Alshahidy and Abbas, 2020). Biodiesel can be easily produced from heterogeneous catalysts by converting fat or oil in a slow way and can be reusable after treatment. Consequently, the production cost of the process is low, and the catalysts are noticed to be characterized by their high activity and stability (Alshahidy and Abbas, 2021).

Calcium oxide, which is a base solid catalyst is widely used as heterogenous catalyst in transesterification reaction because it's cheap, eco-friendly, non-corrosive and can be reused in transesterification reactions (Widayat *et al* 2017). It can be generated from eggshells (Mmusi, Odisitse and Nareetsile, 2021), snail shells (Krishnamurthy, Sridhara and Ananda Kumar, 2020), oyster shells (Lin *et al.*, 2020), fish boon (Sulaiman *et al.*, 2021). Biological synthesis of CaO nanoparticles (NPs) from a green source such as plants containing bioactive coupons such as alkaloids, steroids, and terpenoids, which act as an agent that reduces, is another promising path for the production (Sahu *et al.*, 2023). The limitation of using this catalyst is the FFA content should be less than 3 wt.% and water content 1 wt.% (Mmusi, Odisitse and Nareetsile, 2021).

Calcium is an essential plant nutrient as it plays an important role in the formation of plant cell walls and membranes. Most soils contain large amounts of calcium, which causes the plant to absorb excessive amounts of this mineral, which may be toxic if it accumulates. Therefore, the plant stores the excess calcium in the plant leaves, and it is easily disposed of by shedding the leaves and then getting rid of the excess calcium with the leaves. It has long been acknowledged that phytochemicals found in plants can act as a biological agent to reduce the synthesis of metals and metal oxides (Nair and Jadhav, 2020; Nagore *et al.*, 2021). Several research have utilized plant leaves extracts for the production of calcium oxide. Jadhav *et al.*, (2022) used leaves aqueous extract of Moringa oleifera to produced calcium oxide nanoparticales (CaO NPs). Also, the potential production of CaO nanocatalyst from Acalypha indica leaves was inquiry (Cholapandian, Gurunathan and Rajendran, 2022). Mango tree is a perennial with large leaves. Furthermore, this tree not only possesses aesthetic appeal but also yields significant economic benefits. The tree is highly productive, as its fruits are regarded as a nutrient-rich food source abundant in vitamins and minerals. Multiple research have examined the advantages of extracting mango leaves, revealing their potential as anti-cancer, anti-diabetic, anti-oxidant, anti-microbial, anti-obesity, lipid-lowering, hepato-protective, and anti-diarrheal agent (Kumar *et al.*, 2021). Furthermore, the fallen leaves of this plant can be utilized for the production of calcium oxide and serve as a highly effective catalyst in the transesterification process for biodiesel production. It was found that the calcium present in the mango leaves can be reached to 4.41% (Ali *et al.*, 2020; Kumar *et al.*, 2021). The green approach of mango leaves extract is more cost-effective, nontoxic, and environmentally friendly compared to other ways such as chemical and physical procedures (Jadhav *et al.*, 2022).

Consequently, the current study attempted to extract the calcium found in the fallen leaves of the mango tree and developing a green biosynthesis of CaO NPs by reducing and stabilizing the calcium nitrate precursor, thereafter the ability of the catalyst in the production of biodiesel by transesterification reaction was investigated. In order to optimize the cost of biodiesel production, a waste cooking oil (WCO) was used as raw material. The influence of the temperature, catalyst loading, methanol/oil ratio (weight/weight) (w/w), and time of the reaction on the yield were studied. In addition, the kinetics of the reaction was highlighted.

2.Materials and method

2.1 Chemical

Calcium nitrate tetrahydrate ($Ca(NO_3)_2.4H_2O$) was supplied by Thomas Baker, India with 98% purity, sodium hydroxide (NaOH) was supplied from Thomas Baker, India, methanol purchased from chem-lab NV, Belgium with 99.8+% purity, isopropyl alcohol purchased from Alpha chemika, India with the minimum assay of 99.5%, and deionized water grade-I (extra pure). Phenolphthalein indicator.

2.2 Treatment of waste cooking oil (WCO)

Wast cooking oil (WCO) was purchased from local restaurant in Baghdad (Iraq). First WCO is treated by filtration to remove any impurities and food particles then the properties of the oil are tested such as free fatty acid content (FFA) and water content, FFA content was measured by titration of the oil against 0.1N KOH. The milligram of KOH needs to neutralized all the acid present in the sample will be known as the acid value and FFA is equal to half of the acid value (Nazir *et al.*, 2021). 20 g of oil were mixed with 100 ml of isopropyl alcohol and incorporated a small amount of phenolphthalein indicator then titrated with 0.1N KOH until the colour of the mixture turned to light pink. The FFA% in the oil is the half of the KOH used in titration, which was found to be 1.8%, this percentage of FFA is acceptable to the heterogenous catalyst. The water content is measured by taking a sample of the oil (20 g) and put in the oven at 105 ℃ for 30, 60, and 90 minutes the water content is calculated from the weight loss of the sample, and it's found to be 0.04%.

2.3 Preparation Of Mango Leaves Powder

Mango leaves were collected from local gardens located in Baghdad- Iraq and washed with distilled water, and repeat the rinsing process with deionized water to eliminate any remaining dirt or other unwanted substances. The mango leaves were then dried in the oven at 80 ℃ for 2 hours after that and used a mortar and pestle to create a powder.

2.4 Synthesized of Calcium Oxide Nanoparticles

2 g of mango leaves powder was taken and then heated for 25 in deionized water at 60 ℃. Shows the formation of a solution with a light brown colour. Then the resulting solution was chilled at laboratory temperature, and then the formed solution was filtered by filter paper. The filtrated aqueous was stored in a refrigerator (2 ℃ to 4 ℃) for further work. 20 ml of mango leaves aqueous extract was taken and it's heated to 55 ℃, then 2 g of calcium nitrate tetrahydrate ($Ca(NO_3)_2.4H_2O$) was added to the aqueous and a few drops of (2M NaOH) added to the mixture. The mixture was kept on the heater until it became a yellow-coloured paste. The resulting mixture was filtered by using filter paper the precipitate was calcination for 3h in a muffle furnace up to 700 ℃ and CaO nanoparticles were produced.

2.5 Transesterification reaction

The transesterification reaction was conducted in a 500 mL 3 nick flask using 30g of waste cooking oil (WCO) the experimental apparatus was positioned on a heated plate that was equipped with a magnetic stirrer and the middle neck was fitted with a reflux condenser to condensate the evaporated

methanol and one of the side nicks are connected with a mercury thermometer. Several experiments were carried out at different methanol to oil ratios w/w (30, 40, 50, 60, 70 %) (w/w oil) with constant catalyst content 1g (3.333 wt. %), temperature 65 ℃ , and 1.5 hr. when the higher yield reached the methanol to oil wt.% ratio fixed and start to change the catalyst content with fixed the remaining parameter until reaching the higher yield and fixed the catalyst content and so on the other parameter. The reaction product was left to settle overnight and then three layers appeared the lower layer catalyst, the middle layer glycerol and the upper layer biodiesel which was collected then separated from the catalyst by centrifuge and then put in the dryer for 24 hr on 65 ℃ to evaporate the remaining methanol then the yield was calculated by the equation below (Sahu *et al.*, 2023).

$$Yield\ (\%) = \frac{Weight\ of\ biodiesl}{Weight\ of\ oil} * 100$$

2.6 Catalyst regeneration

Following each catalytic experiment, the catalyst was separated and collected from the product and then regenerated by washing it with methanol and hexane. Subsequently, it was dried in an oven at 75 ℃ for 5 hours. Then the transesterification reaction of the regeneration catalyst was carried out while maintaining optimal reaction conditions, including a 50 wt.% methanol to oil ratio, a reaction period of 1.5 hours, a temperature of 65 ◦C, and a catalyst content of 3 wt.%.

2.7 reaction kinetic

The scheme of the conversion of triglyceride to fatty acid methyl ester according to equation (1) (Foroutan, Mohammadi and Ramavandi, 2021):

$$TG + 3ROH \leftrightarrow 3R'CO_2R + GL \quad (1)$$

The reaction will be assumed to be irreversible since the mole concentration of methanol is excess over the product in earlier reaction time, the excess methanol over the other reactant will make second order reaction act like a first-order reaction (Mercy Nisha Pauline *et al.*, 2021), according to that the reaction will be:

$$A + B \rightarrow Product \quad (2)$$

C_{Bo} methanol is higher than C_{Ao} triglyceride, so C_B remains constant at all times the reaction will be:

$$A \rightarrow Product \quad (3)$$

The rate of the reaction can be written as follows:

$$-r_a = k\ C_A \quad (4)$$

Rate constant can be calculated by observing the conversion at different time by using eq. (5)

$$-\ln(1-X_A) = kt \quad (5)$$

Where (X_A) is the yield of biodiesel, (k) is the rate constant and (t) is the reaction time.
The Arrhenius equation is utilized to calculate the activation energy and pre-exponential factor (A) of the transesterification reaction.

$$k = Ae^{-Ea/RT} \quad (6)$$

or

$$\ln k = \ln A - Ea/RT \quad (7)$$

Where A is the pre-exponential factor, Ea is the activation energy of reaction J/mol, R is gas constant 8.314 J/mol.K and T is the reaction temperature in K.

3. Result and discussion

3.1 Characterization of mango leaves extract

To inspect the presence of biomolecules (metabolites) which consist of different functional groups (-OH, -COOH, -NH, C=O, -SH) which serve as natural reducing, capping and stabilizing agents for nanocatalyst synthesis, the mango leaves extract was analyzed by FT-IR. Figure 1 shows the vibration banded at 3446.56 and 2923.88 cm^{-1} are assigned to N-H stretching of amides and C-H stretching, respectively. O-H stretching of carboxylic acids and C=C stretching in alkene are assigned in vibration bands 2856.38 and 1631.67 cm^{-1}. 1400.22 cm^{-1} (symmetric stretching of carboxyl side groups of amino acid residue), 1263.29 cm^{-1} amide III band of protein (Stani *et al.*, 2020), 1033.77 cm^{-1} C=N (vibration of amine), 619.11 cm^{-1} (strong C-halo, alkyl halide). These bands verify the existence of metabolites such as tocopherols, tocotrienols, phenolic acids, carbohydrates and phenolic alkaloids in the extract. The ability of C=O groups of amino acid protein to act as reducing and capping agents at the surface of produced CaO or $Ca(OH)_2$ is shown by the reduction of calcium nitrate to calcium hydroxide or calcium oxide (Al-Mohaimeed, Al-Onazi and El-Tohamy, 2022; Sahu et al., 2023).

3.2 EDS analysis of mango leaves extract

The mango leaves extract was characterized by EDS analysis to investigate the element present in the extract and their quantities, 10 ml of extract was taking and analysis. The EDS spectrum depicted in Figure 2 illustrates the presence of many elements in the extract of fallen mango leaves. These elements include calcium (7.1 wt.%), oxygen (55.8 wt.%), carbon (28.5 wt.%), sodium (6.6 wt.%), magnesium (1.6 wt.%), and potassium (0.4 wt.%). The EDS analysis reveals a significant presence of carbon and oxygen in the extract, which are commonly present in organic substances like leaves. Additionally, calcium, which plays a crucial role in cell wall formation and stability, was detected in a significant concentration in the fallen mango leaves extract, indicating its potential for used of mango leaves as source of calcium. Carbon, sodium and other element will be eliminated during the calcination process at a temperature of 700 ℃. This was confirmed by the XRF and EDS analysis of the resulting nanocatalyst.

3.3 XRF analysis

The produced CaO nanocatalyst from the calcination process was characterized using XRF spectrometry (type spectrum

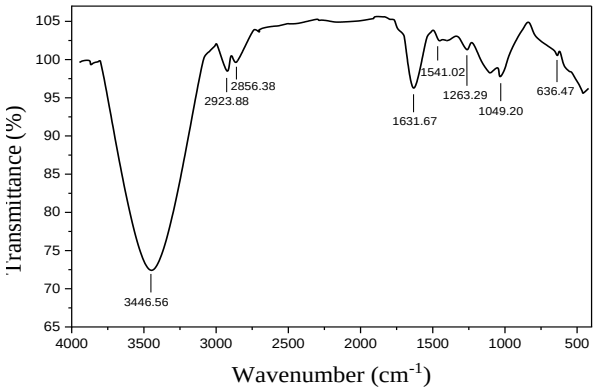

Fig. 1. FT-IR analysis for mango leaves extract.

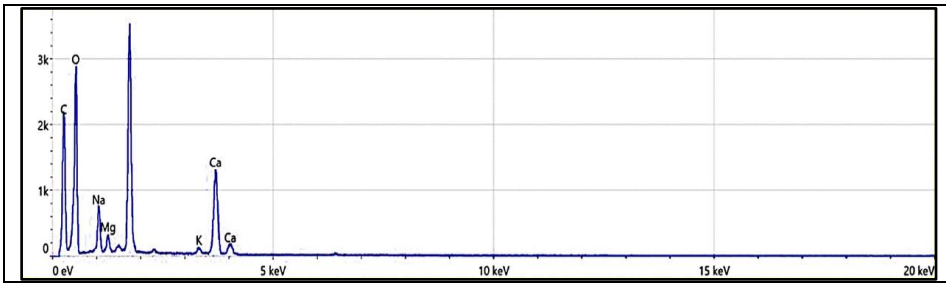

Element	Weight %
C	28.5
O	55.8
Na	6.6
Mg	1.6
K	0.4
Ca	7.1

Fig. 2. EDS analysis of mango leaves extract.

Table 1
XRF analysis of the produced catalyst.

Component	Wt.%	Component	Wt.%
CaO	98.66	SrO	0.01239
MgO	0.0425	I	0.00657
SiO_2	0.698	Te	0.008419
SO_3	0.0601	Rb_2O	<0.0000346
Cl	0.047	Al_2O_3	<0.004382
P_2O_5	0.3677	K_2O	<0.007612
Ag	0.0025	MnO	0.0012226

Xepos, Ametek). An X-ray fluorescence (XRF) spectrometer is used to accurately identify and measure the amounts of different elements present in CaO the chemical composition of the prepared catalyst was shown in Table 1. The XRF analysis detected the presence of the substances P_2O_5 and SiO_2 at concentrations of 0.3677% and 0.698%, respectively. Calcium oxide (CaO) comprises the predominant component, accounting for 98.66%. And another element such as MgO, SrO, I, etc. were found in trace amount. The inclusion of this element does not alter the structural properties of the CaO nanocatalyst.

3.4 X-ray diffraction (XRD) analysis

To check the crystal size, structure, composition and degree of crystallization of CaO NPs X-ray powder diffraction mechanics were used. Figure 3 displays the X-ray diffraction (XRD) profile of the CaO nanocatalyst. The presence of well-defined diffraction peaks indicates the high-quality crystallinity of the catalyst. The most prominent peak is detected at the Bragg's angle of 2θ = 32.29°, 37.47°, 54.09°, 64.43°, 67.64°, corresponding to the Miller indexes (111), (200), (202), (311), and (222) respectively, indicating the crystallization of the catalyst. These results corroborate that $Ca(OH)_2$ is transformed into CaO which improves the transesterification process of waste cooking oil. The detection of very faint peaks suggests the presence of trace amounts of $CaCO_3$. The average crystal size of the CaO nanocatalyst was determined to be 24.650 nm using the Debye-Scherrer equation, and previous reports in the literature also indicated peaks with a similar shape.

3.5 Fourier transform infrared (FT-IR) spectroscopic.

The FT-IR spectroscopic of the manufactured CaO nanocatalyst shown in Figure 4 is used to analyse the functional groups in the

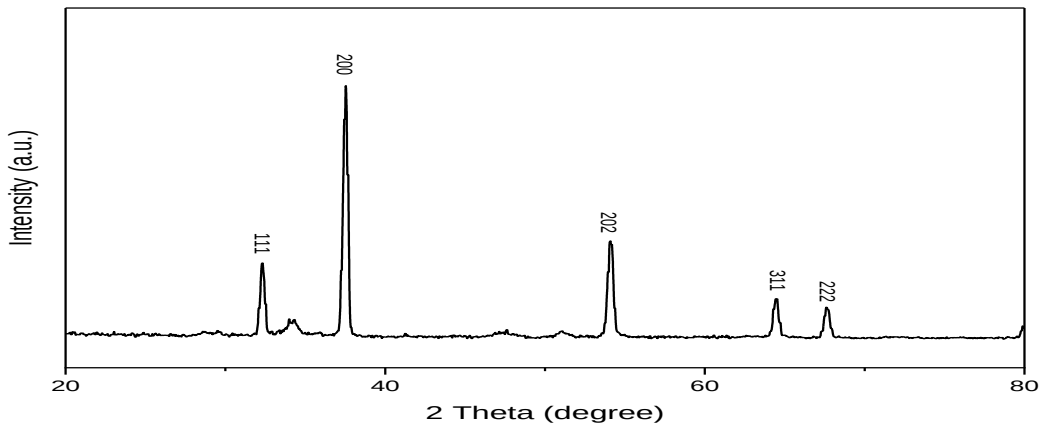

Fig. 3. XRD analysis.

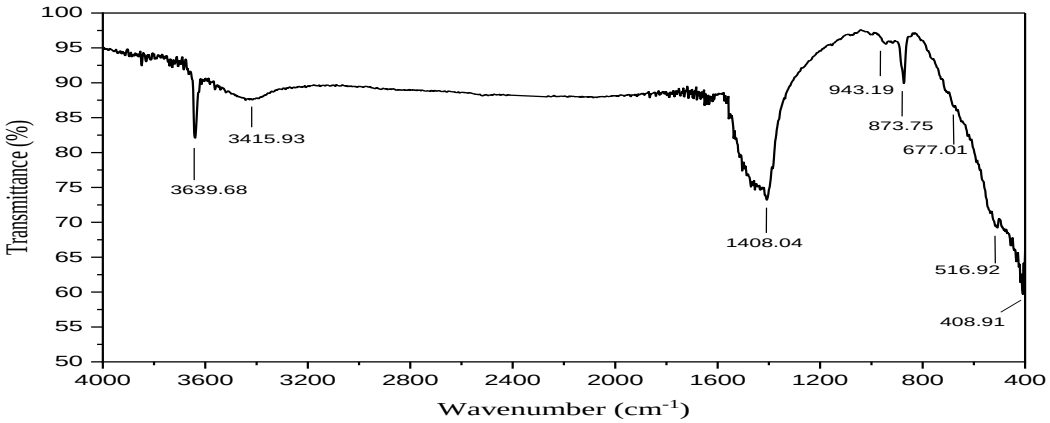

Fig. 4. FT-IR of manufacture CaO nanocatalyst.

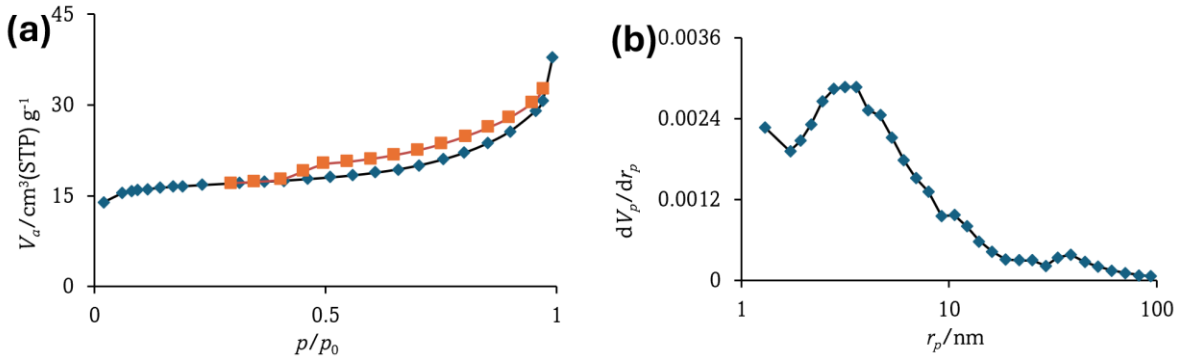

Fig. 5. (a) The isotherm adsorption-desorption nitrogen. (b) Distribution of pore size of produced CaO nanocatalyst.

catalyst. The IR spectrum of the manufactured catalyst was recorded at 400-4000 cm^{-1}. Figure 4 shows that the most adsorption bands appear at 3639.68, 1408.04 cm^{-1}, 943.19 cm^{-1}, 873.75 cm^{-1}, 677.01 cm^{-1}, 516.92 cm^{-1}, 408.91 cm^{-1}. Abroad peak around 3639.68 refers to (O-H) hydroxyl group stretching vibration, and it's due to the H_2O molecule's physical adsorption on the synthesis CaO surface (Pandit and Fulekar, 2019; Vinoth Arul Raj *et al.*, 2021) this shows that the water is not the reason for the deactivation of the catalyst. The spectra obtained at 1408.04 cm^{-1} refer to the presence of CO_3^{-2} species (Vinoth Arul Raj *et al.*, 2021) and the absorption peak at 873.75 cm^{-1} shows the O-C-O functional group (Krishnamurthy, Sridhara and Ananda Kumar, 2020; Sivanesh *et al.*, 2022). The spectra at 516.92 cm^{-1} appear as a result of the stretching vibration frequency of Ca-O bonds (Ramola and Joshi, 2019; Changmai *et al.*, 2021) and the peak at 943.19 cm^{-1} directs the occurrence of Si-O-Si stretching as a small amount of silica was present.

3.6 BET analysis

BET was used to determine the average pore diameter, isotherm adsorption-desorption nitrogen, total pore volume and the specific surface area of the synthesis CaO nanocatalyst calcined at 700 ℃ as shown in Figures 5a and 5b. The mesoporous material is observed from a typical type IV characteristics curve in the isotherm. The manufacturer CaO has BET specific surface area of 64.989 $m^2 g^{-1}$ with a pore volume of 0.057623 $cm^3 g^{-1}$ and an average pore diameter of 3.5466 nm. Most of the average pore diameters are in the range of 2-10 nm so the transesterification reaction will simply occur by the penetration of triglyceride molecules (Krishnamurthy, Sridhara and Ananda Kumar, 2020).

3.7 SEM-EDS analysis

A scanning electron microscope (SEM) equipped with energy-dispersive X-ray spectroscopy (EDX) was utilized to examine the quantitative and qualitative elemental composition of the surface structure of the CaO nanocatalyst generated. The CaO nanocatalyst SEM images are shown in Figures 6a, 6b, and 6c it was illustrated by using a magnification of 1 µm, 2 µm, and 200 nm respectively. The scanning electron microscope (SEM) image reveals a limited number of shapeless structures that are spherical. These structures exhibit significant clustering of the catalyst particles, it can be ascribed to their extensive surface area. The catalyst made of nano CaO has a multi-pore structure characterized by three distinct crystallographic surfaces, which offer several active sites for catalytic activity (Sahu *et al.*, 2023). Figure 6d displayed the EDS spectra of the CaO nanocatalyst. The analysis revealed that calcium (46.11%) and oxyen (51.95%) were found in greater quantities and The CaO nanocatalyst derived from mango leaves contains minor amounts of Na (1.65%), and Si (0.29%). The catalyst's EDS examination confirms a significant concentration of Ca and O, resulting in a very alkaline nature that enhances the transesterification process of waste cooking oil.

3.8 Effects of reaction parameters

3.8.1 The impact of methanol to waste cooking oil WCO ratio (wt.%)

Biodiesel production is affected by the methanol/oil (weight/weight) (w/w) ratio. Methanol is the smallest chain

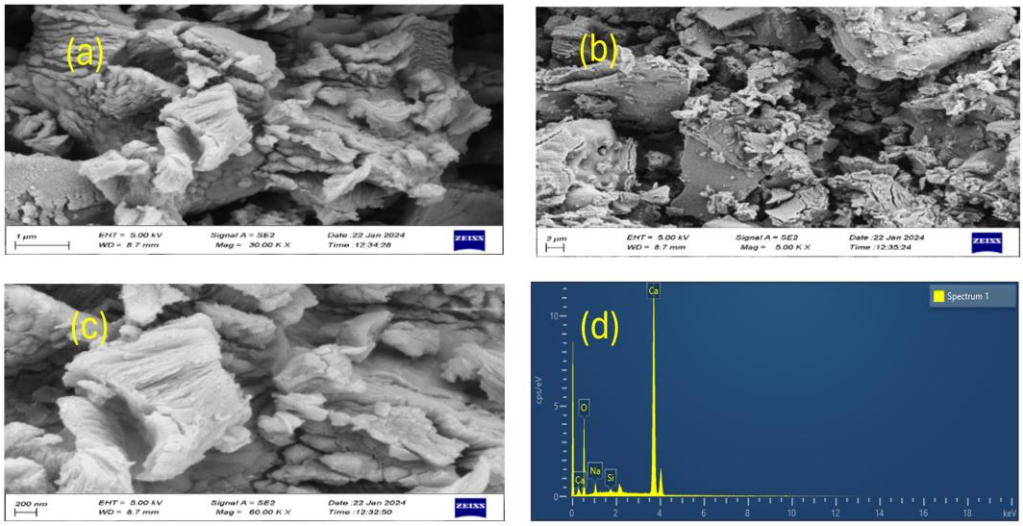

Fig. 6. SEM-EDS analysis.

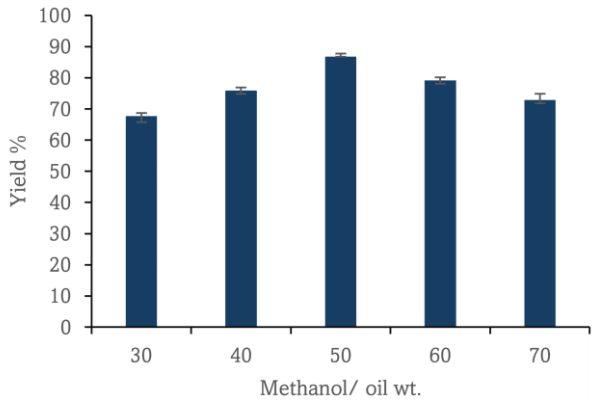

Fig. 7. Effect of methanol to oil (w/w) ratio at a fixed catalyst content 3.33 wt.%, temperature 65℃ , time 1.5 hr.

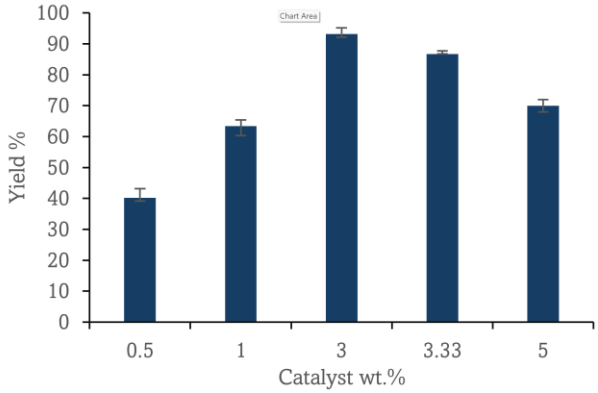

Fig. 8. Effect of catalyst content at fixed methanol /oil ratio 50 wt.%, temperature 65℃, time 1.5 hr.

length of any alcohol. It provides a more stable product and a higher yield rate than longer-chain alcohol (Seffati *et al.*, 2019). Since the stoichiometric ratio between methanol and triglyceride is 3:1, and to favour the synthesis of biodiesel, an excess of methanol is necessary due to the reversible nature of the transesterification reaction. The current study examined the impact of the methanol/oil weight ratio within the range of 30-70%. Other parameters, such as a fixed temperature of 65 °C, a reaction time of 1.5 hours, and a catalyst content of 3.33 wt.%, remained constant. The results demonstrated that the maximum yield of 86.745% was obtained at a ratio of 50% as shown in Figure 7. Further increasing of the methanol/oil ratio to 70% causes the yield to decrease to 72.85%, which might be due to an excessive quantity of methanol might dissolve the by-product glycerol, resulting in complications during the separation process Therefore, once the optimal ratio is reached, the reaction will shift in the opposite direction (Hussien and Abdul hameed, 2019).

3.8.2 The impact of catalyst loading

The effluence of catalyst loading plays a crucial role in the production of biodiesel, transesterification reaction was obtained using different ranges of catalyst (0.5-5) wt.%. with fixed other parameters such as temperature of 65 °C, reaction time of 1.5 h, and methanol /oil ratio of 50% (w/w). The results illustrated in Figure 8 show that by increasing the catalyst percentage from 0.5% to 3% the yield increased from 40.21% until it reached a maximum value of 93.21%, further increasing resulted in a reduction of the yield where the yield of biodiesel reduced to (69.998%) as the catalyst percentage increased to (5%). That could be attributed to the limitation in mass transfer and high saponification reaction leads to a decrease in the production of biodiesel and makes it more difficult to separate the components ultimately reducing the biodiesel output (Seffati *et al.*, 2019).

3.8.3 The impact of reaction temperature

The effect of reaction temperature was studied at different ranges (55-70) ℃ in the production of biodiesel under other constant conditions such as 1.5 h reaction time 50% methanol/oil ratio w/w, and 3 wt.% catalyst loading. Figure 9 shows that the yield increased linearly with the temperature from 77.8253% at 55 ℃ to 84.6585 at 60℃ until it reached the maximum yield of 93.21% at 65 ℃ further increased in temperature causing the yield of biodiesel to decrease to 88.372% at 70 ℃. The decrease in methanol concentration due to evaporation and the increase in reaction temperature both promoted the saponification reaction of the triglyceride (TG) (Hussien and Abdul hameed, 2019). So, 65 °C was considered the optimum value.

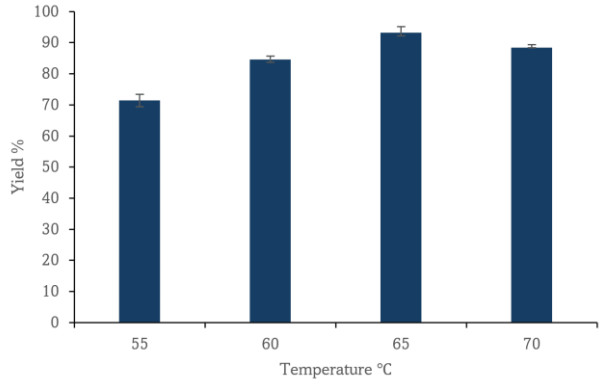

Fig. 9. Effect of temperature at fixed methanol to oil ratio 50 wt.%, catalyst 3%, time 1.5 hr.

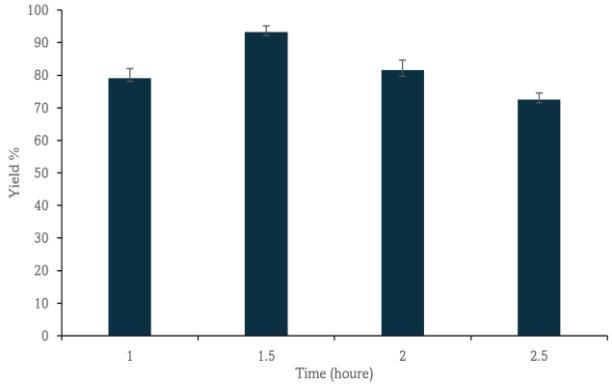

Fig. 10. Effect of time at fixed methanol to oil ratio 50 wt.%, temperature 65 °C, catalyst 3%.

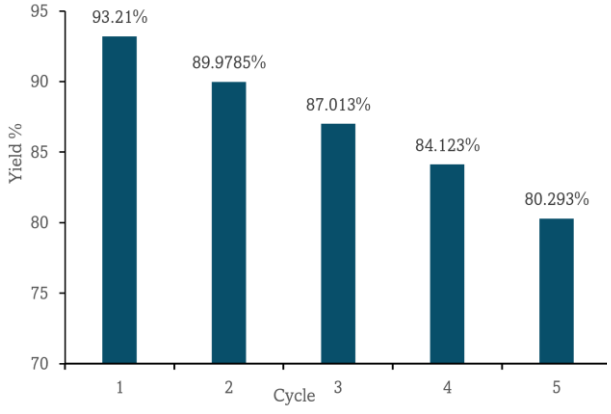

Fig. 11. The reusability of catalyst

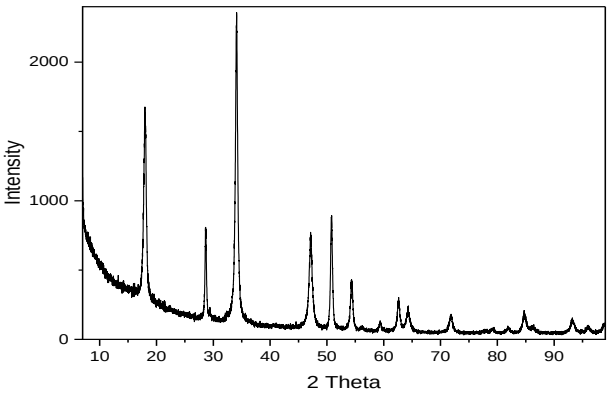

Fig. 12. The XRD analysis of reused CaO after the 5th cycle.

3.8.4 The impact of reaction time

The reaction time in transesterification is regarded to be the most critical parameter of the effect of the time study under constant conditions of methanol to oil ratio of 50% w/w, temperature of 65 °C, and catalyst loading of 3 wt.%. In this study, different reaction times of 60, 90,120, and 150 minutes have been studied. Figure 10 shows that the biodiesel yield of the transesterification reaction increases with time it's augmented from 83.887% at 60 min. Until it's reached the maximum yield of 93.21% at 90 min. which is the optimum point then the yield. Thereafter, it decreased to 81.631 % after 120 min. of operation. Furthermore, the yield decreased to 72.559% after 150 minutes. The decrease in yield may be attributed to the occurrence of a reverse reaction, which leads to the formation of soap due to an excess of fatty acids.

3.9 Catalyst reusability

The heterogeneous catalysts are typically associated with industrial applications due to their reusability property of the catalyst which is considered the core of the process feasibility, where it increases the overall value of the process (Aleman-Ramirez *et al.*, 2021). The investigation involved assessing the catalyst's ability to be reused. Figure 11 shows that, by repeatedly using the catalyst, a decrease in biodiesel production on the 5th cycle until it reached 80.293%. The reduction in productivity occurred due to the accumulation of organic compounds within the reaction mixture (Rozina *et al.*, 2022). Repeated washing can restore the catalytic activity of CaO nanoparticles. This occurs due to the contamination of the active sites of the nanoparticles, resulting in a reduction in the volume of pores and the overall surface area of the particles Consequently, the effectiveness of the catalyst is reduce (LaGrow *et al.*, 2019). The XRD measurement in Figure 12 verified the presence of the crystalline phase of the catalyst after the reaction as the main peaks of CaO nanocatalyst are still exist 2θ =34.06°, 54.303°, 64.241°. Upon examination, it was discovered that the catalyst, which had been used 5 times, still had the distinctive CaO phase. Appearance of peaks at 2θ = 28.64°, 47.102°, 50.768°, 56.1922° in the diffraction patterns of the reused catalyst confirmed the presence of hexagonal calcium carbonate as a significant phase. The creation of calcium carbonate may result from the interaction between calcium hydroxide and ambient CO2, which occurs during the repetitive use of a catalyst and the process of drying. Hence, the decline in fundamental potency and alterations in structure are the main factors accountable for the decrease in catalytic efficacy after its repeated utilization (Praikaew *et al.*, 2022).

3.10 Kinetic study of transesterification reaction

The kinetics of the transesterification reaction was studied at various temperatures of 55, 60, 65, and 70 °C with a constant methanol-to-oil ratio of 50% (w/w) and a catalyst content of 3%, the experiment ran for 15, 30, 45, 60, and 90 minutes.

In Figure 13a, the term -ln(1- X_A) is plotted versus the response time of 15-90 min. At different temperatures 55–70 °C. The transesterification reaction is found to be a pseudo-first-order reaction kinetics as it gives a linear relationship between

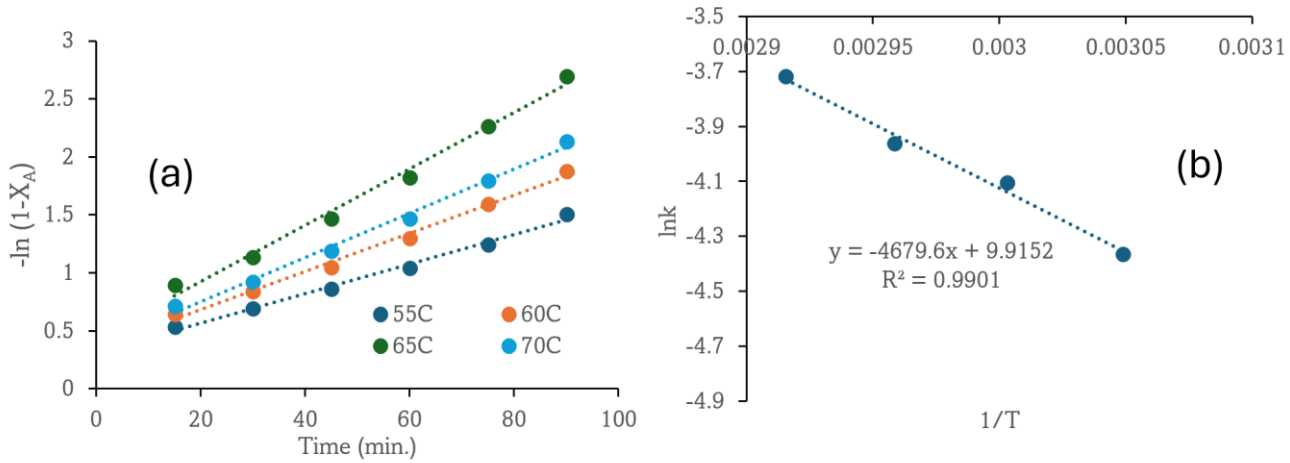

Fig. 13. (a) -ln(1-X_A) vs time. (b) lnk vs 1/T.

Table 2
Rate constant of transesterification reaction

Temperature	K	R^2
55°C	0.012725226	0.9911
60°C	0.016494913	0.9931
65°C	0.024244872	0.9901
70°C	0.019079433	0.9931

-ln(1- X_A) and time. Table 2 show rate constant for irreversible first order reaction, the findings of this study clearly indicate that the rate of the transesterification process is influenced by temperature, as seen by the rise in the rate constant (k) as the temperature increases from 55°C to 65°C. This phenomenon is consistent with the laws of chemical kinetics, wherein a rise in temperature generally leads to an elevated reaction rate as a result of the heightened kinetic energy of the molecules participating in the reaction. Nevertheless, the rate constant at 70°C was seen to be somewhat lower than at 65°C, which contradicts the anticipated pattern. This anomaly may be ascribed to several sources, such as potential thermal deterioration of the reactants or products at higher temperatures, a change in the reaction mechanism, or the initiation of a reversible process that becomes significant at increasing temperatures.

As depicted in Figure 13b the pre-exponential factor (A) represents the intercept of the plot between (ln k) vs. (T^{-1}), and the activation energy can be determined from the slope (-Ea/R). the activation energy of the reaction obtained from the figure was 38.906 kJ mol^{-1}, which is within the range of activation energy for oil transesterification 21–84 KJ mol^{-1} (Zhang *et al.*, 2020). This implies that the reaction necessitates a moderate amount of energy to advance, rendering it achievable under standard laboratory or industrial circumstances. When comparing this number with existing research, it aligns with the published activation energies for transesterification processes that include similar reactants and catalysts. The results of this study have important practical implications for improving transesterification processes, especially in the context of biodiesel production. By carefully managing the reaction temperature, it is possible to achieve higher conversion rates and perhaps reduce production costs. Potential future research might entail investigating the impact of various catalysts or solvent systems in order to further decrease the activation energy and enhance the efficiency of the process.

Table 3 demonstrates a comparison of the best conditions adopted for the production of biodiesel from different feedstock utilizing CaO as a catalyst. It can be observed that the present work produced biodiesel with 93.21% yield at a temperature of 65 °C, 50% w/w methanol /oil, 3 wt.% catalyst and with a reaction time of 90 min. which considers higher yield in good condition compared to another study. However, Amesho et al., (Lin *et al.*, 2020) produced biodiesel from WCO using CaO driven from oyster shell scallops with a maximum yield of

Table 3
Comparison of production of biodiesel by using CaO.

Feedstock (Oil)	Catalyst source	Meth/oil Molar ratio	Temperature	Catalyst (wt%)	Reaction time (min.)	Yield % (wt%)	Ref.
WCO	Mango leave (NPs)	12.67:1	65 °C	3	90	93.21	Current study
WCO	Waste oyster shell	9:1	65 °C	6	180	87.3	(Lin *et al.*, 2020)
Soybean	Watermelon peel (NPs)	20:1	65 °C	8	150	96.2	(Sahu *et al.*, 2023)
Palm	Fishbone	18:1	65 °C	10	240	90.0	(Sulaiman *et al.*, 2021)
WCO	Mussel shell	9:1	65 °C	10	180	89.0	(Rosdzimin, Rahim and Author, 2020)
WCO	Donax deltoides shell	63:8	65 °C	7.5	129	96.5	(Niju, Vishnupriya and Balajii, 2019)
WCO	Malleus malleus shell	12:1	65 °C	7.5	86	93.8	(Niju *et al.*, 2020)

87.3%, but it needed a higher catalyst concentration of 6 wt.% and a longer reaction time of 180 min. In addition, Sulaiman et al., (Sulaiman *et al.*, 2021) produced 90% biodiesel using CaO driven from fish bone and palm oil but it was achieved by using 10 wt.% catalyst and 240 min. reaction time. Biodiesel can be produced from watermelon peel as in the work of Sahu et al., (Sahu *et al.*, 2023) with 96.2% yield and 8 wt.% catalyst concentration, 150 min. reaction time which is considered more than double the time this study needed and more than double the catalyst concentration, Table 3 shows that this study produced 93.21% biodiesel.

4. Conclusion

The present study successfully prepared a CaO nanocatalyst using mango leaf extract. X-ray diffraction (XRD) analysis confirmed that the synthesized catalyst exhibited a nano-sized structure. The catalyst underwent testing and exhibited significant catalytic activity in the transesterification reaction of biodiesel derived from waste cooking oil, achieving a yield rate of 93.21% under optimal conditions of 1.5 hours reaction time, 65°C temperature, 3% catalyst concentration, and a 50% methanol to oil weight ratio. The activation energy was found to be 38.906 KJ/mol which is necessary to break the energy barrier and start the transesterification process and the reaction was first order. The CaO nanocatalyst demonstrated a consistently high yield of 80.293% even after the 5th reaction cycle, indicating its superior stability. The production cost of biodiesel can be reduced due to the catalyst's exceptional reusability, allowing it to be utilized in multiple reaction cycles. The catalyst can be employed for the large-scale production of biodiesel from oils in an industrial setting.

References

Abdul-Kader, H.A., Shakor, Z.M., Sherhan, B.Y., Al-Humairi, S.T., Aboughaly, M., Hazrzt, M.A. and Fattah, I. M. R. (2023) Biodiesel production from waste cooking oil using KOH / HY-type nano-catalyst derived from silica sand, *Biofuels*, 0(0), 1–17. Available at: https://doi.org/10.1080/17597269.2023.2267849 .

Abd, M.F. and Al-Yaqoobi, A.M. (2023) The feasibility of utilizing microwave-assisted pyrolysis for Albizia branches biomass conversion into biofuel productions, *International Journal of Renewable Energy Development*, 12(6), 1061–1069. Available at: https://doi.org/10.14710/ijred.2023.56907 .

Abd, M.F. and AL-yaqoobi, A.M. (2024) The Potential Significance of Microwave-Assisted Catalytic Pyrolysis for Valuable Bio-Products Driven from Albizia Tree, *Applied Science and Engineering Progress* [Preprint]. Available at: https://doi.org/10.14416/j.asep.2024.07.016 .

Abd, M.F., Al-yaqoobi, A.M. and Abdul-Majeed, W.S. (2024) Catalytic Microwave Pyrolysis of Albizia Branches Using Iraqi Bentonite Clays, *Iraqi Journal of Chemical and Petroleum Engineering*, 25(2), 175–186. Available at: https://doi.org/10.31699/ijcpe.2024.2.16 .

Al-Mohaimeed, A.M., Al-Onazi, W.A. and El-Tohamy, M.F. (2022) Multifunctional Eco-Friendly Synthesis of ZnO Nanoparticles in Biomedical Applications, *Molecules*, 27(2), 579. Available at: https://doi.org/10.3390/molecules27020579 .

Al-Yaqoobi, A., Al-Rikabey, M. and Al-Mashhadani, M. (2021) Electrochemical harvesting of microalgae: Parametric and cost-effectivity comparative investigation, *Chemical Industry and Chemical Engineering Quarterly,* 27(2), 121–130. Available at: https://doi.org/10.2298/CICEQ191213031A .

Aleman-Ramirez, J.L., Moreira, J., Torres-Arellano, S., Longoria, A., Okoye, P.U. and Sebastian, P.J. (2021) Preparation of a heterogeneous catalyst from moringa leaves as a sustainable precursor for biodiesel production, *Fuel,* 284. Available at: https://doi.org/10.1016/j.fuel.2020.118983 .

Ali Abbas, R. and M. Flayeh, H. (2019) Bioethanol (Biofuel) Production from Low Grade Dates, *Iraqi Journal of Chemical and Petroleum Engineering*, 20(4), 41–47. Available at: https://doi.org/10.31699/ijcpe.2019.4.7 .

Ali, B.A., Alfa, A.A., Tijani, K.B., Idris, E.T., Unoyiza, U.S. and Junaidu, Y. (2020) Nutritional Health Benefits and Bioactive Compounds of Mangifera indica L (Mango) Leaves Methanolic Extracts, *Asian Plant Research Journal,* 41–51. Available at: https://doi.org/10.9734/aprj/2020/v6i230126 .

Alshahidy, B.A. and Abbas, A.S. (2020) Preparation and modification of 13X zeolite as a heterogeneous catalyst for esterification of oleic acid, *AIP Conference Proceedings*, 2213(March). Available at: https://doi.org/10.1063/5.0000171 .

Alshahidy, B.A. and Abbas, A.S. (2021) Comparative study on the catalytic performance of a 13X zeolite and its dealuminated derivative for biodiesel production, *Bulletin of Chemical Reaction Engineering and Catalysis*, 16(4), 763–772. Available at: https://doi.org/10.9767/bcrec.16.4.11436.763-772 .

Changmai, B., Vanlalveni, C., Ingle, A.P., Bhagat, R. and Rokhum, S.L. (2020) Widely used catalysts in biodiesel production: A review, *RSC Advances,* 10(68), 41625–41679. Available at: https://doi.org/10.1039/d0ra07931f.

Changmai, B., Rano, R., Vanlalveni, C. and Rokhum, S.L. (2021) A novel Citrus sinensis peel ash coated magnetic nanoparticles as an easily recoverable solid catalyst for biodiesel production, *Fuel,* 286, 119447. Available at: https://doi.org/10.1016/j.fuel.2020.119447 .

Cholapandian, K., Gurunathan, B. and Rajendran, N. (2022) Investigation of CaO nanocatalyst synthesized from Acalypha indica leaves and its application in biodiesel production using waste cooking oil, *Fuel,* 312, 122958. Available at: https://doi.org/10.1016/j.fuel.2021.122958 .

Foroutan, R., Mohammadi, R. and Ramavandi, B. (2021) Waste glass catalyst for biodiesel production from waste chicken fat: Optimization by RSM and ANNs and toxicity assessment, *Fuel,* 291, 120151. Available at: https://doi.org/10.1016/j.fuel.2021.120151 .

Hadiyanto, H., Lestari, S.P., Abdullah, A., Widayat, W., Sutanto H. (2016). The development of fly ash-supported CaO derived from mollusk shell of *Anadara granosa* and *Paphia undulata* as heterogeneous CaO catalyst in biodiesel synthesis. *Int J Energy Environ Eng* 7, 297–305. https://doi.org/10.1007/s40095-016-0212-6

Hussien, M. and Abdul hameed, H. (2019) Biodiesel production from used vegetable oil (sunflower cooking oil) using eggshell as bio catalyst, *Iraqi Journal of Chemical and Petroleum Engineering*, 20(4), pp. 21–25. Available at: https://doi.org/10.31699/ijcpe.2019.4.4.

Igwe, C.I. (2021) Geothermal Energy: A Review, *International Journal of Engineering Research and Technology*, 10(3), 655–661. Available at: www.ijert.org .

Jadhav, V., Bhagare, A., Wahab, S., Lokhande, D., Vaidya, C., Dhayagude, A., Khaild, M., Aher, J., Mezni, A. and Dutta, M. (2022) Green Synthesized Calcium Oxide Nanoparticles (CaO NPs) Using Leaves Aqueous Extract of Moringa oleifera and Evaluation of Their Antibacterial Activities, *Journal of Nanomaterials*, 2022, 1–7. Available at: https://doi.org/10.1155/2022/9047507 .

Jurmot, S. and Abbas, A.S. (2022) Kinetics and Activation Complex Thermodynamic Study of the Acidity Removal of Oleic Acid via Esterification Reaction on Commercial 13X Zeolite, *Iraqi Journal of Chemical and Petroleum Engineering,* 23(3), 43–49. Available at: https://doi.org/10.31699/ijcpe.2022.3.6 .

Krishnamurthy, K.N., Sridhara, S.N. and Ananda Kumar, C.S. (2020) Optimization and kinetic study of biodiesel production from Hydnocarpus wightiana oil and dairy waste scum using snail shell CaO nano catalyst, *Renewable Energy*, 146, 280–296. Available at: https://doi.org/10.1016/j.renene.2019.06.161 .

Kumar, M., Saurabh, V., Tomar, M., Hasan, M., Changan, S., Sasi, M., Maheshwari, C., Prajapati, U., Singh, S., Prajapat, R.K., Dhumal, S., Punia, S., Amarowicz, R. and Mekhemar, M. (2021) Mango (Mangifera indica l.) leaves: Nutritional composition, phytochemical profile, and health-promoting bioactivities, *Antioxidants,* 10(2), 1–23. Available at: https://doi.org/10.3390/antiox10020299 .

LaGrow, A.P., Besenhard, M.O., Hodzic, A., Sergides, A., Bogart, L.K., Gavriilidis, A. and Thanh, N.T.K. (2019) Unravelling the growth mechanism of the co-precipitation of iron oxide nanoparticles with the aid of synchrotron X-Ray diffraction in solution, *Nanoscale,*

11(14), 6620–6628. Available at: https://doi.org/10.1039/C9NR00531E .
Lin, Y.C., Amesho, K.T.T., Chen, C.E., Cheng, P.C. and Chou, F.C. (2020) A cleaner process for green biodiesel synthesis from waste cooking oil using recycled waste oyster shells as a sustainable base heterogeneous catalyst under the microwave heating system, *Sustainable Chemistry and Pharmacy,* 17. Available at: https://doi.org/10.1016/j.scp.2020.100310 .
Maka, A.O.M. and Alabid, J.M. (2022) 'Solar energy technology and its roles in sustainable development', *Clean Energy*, 6(3), 476–483. Available at: https://doi.org/10.1093/ce/zkac023 .
Masood Ahmad, M., Kumar, A. and Ranjan, R. (2022) Recent Developments of Tidal Energy as Renewable Energy: An Overview. In: Jha, R., Singh, V.P., Singh, V., Roy, L., Thendiyath, R. (eds) River and Coastal Engineering. Water Science and Technology Library, vol 117. Springer, Cham. Available at: https://doi.org/10.1007/978-3-031-05057-2_29 .
Mercy Nisha Pauline, J., Sivaramakrishnan, R., Pugazhendhi, A., Anbarasan, T. and Achary, A. (2021) Transesterification kinetics of waste cooking oil and its diesel engine performance, *Fuel,* 285. Available at: https://doi.org/10.1016/j.fuel.2020.119108 .
Mmusi, K.C., Odisitse, S. and Nareetsile, F. (2021) Comparison of CaO-NPs and Chicken Eggshell-Derived CaO in the Production of Biodiesel from Schinziophyton rautanenii (Mongongo) Nut Oil. Journal of Chemistry, 2021. Available at: https://doi.org/10.1155/2021/6663722 .
Nagore, P., Ghotekar, S., Mane, K., Ghoti, A., Bilal, M. and Roy, A. (2021) Structural Properties and Antimicrobial Activities of Polyalthia longifolia Leaf Extract-Mediated CuO Nanoparticles, *BioNanoScience,* 11(2), 579–589. Available at: https://doi.org/10.1007/s12668-021-00851-4 .
Nair, S.G. and Jadhav, V.R. (2020) Biosynthesis of Silver nanoparticles and comparing its Antifungal property with Ethanolic extract of Ixora coccinea plant, *Asian Journal of Research in Chemistry*, 13(3),198. Available at: https://doi.org/10.5958/0974-4150.2020.00038.3 .
Nazir, M.H., Ayoub, M., Shamsuddin, R.B., Zahid, I. and Zulqarnain (2021) Sulfonated Activated Sugarcane Bagasse as Heterogeneous Catalyst for Biodiesel Production From Waste Cooking Oil via Microwave Irradiation, *200(ICoST),*. 286–291. Available at: https://doi.org/10.2991/aer.k.201229.037 .
Niju, S., Rabia, R., Devi, K.S., Kumar, M.N. and Balajii, M. (2020) Modified Malleus malleus Shells for Biodiesel Production from Waste Cooking Oil: An Optimization Study Using Box–Behnken Design, *Waste and Biomass Valorization*, 11(3), 793–806. Available at: https://doi.org/10.1007/s12649-018-0520-6 .
Niju, S., Vishnupriya, G. and Balajii, M. (2019) Process optimization of Calophyllum inophyllum-waste cooking oil mixture for biodiesel production using Donax deltoides shells as heterogeneous catalyst, *Sustainable Environment Research*, 1(1), pp. 1–12. Available at: https://doi.org/10.1186/s42834-019-0015-6 .
Pandit, P.R. and Fulekar, M.H. (2019) Biodiesel production from microalgal biomass using CaO catalyst synthesized from natural waste material, *Renewable Energy, 136*, 837–845. Available at: https://doi.org/10.1016/j.renene.2019.01.047 .
Praikaew, W., Kiatkittipong, W., Aiouache, F., Najdanovic-Visak, V., Termtanun, M., Lim, W.J., Lam, S.S., Kiatkittipong, K., Laosiripojana, N., Boonyasuwat, S. and Assabumrungrat, S. (2022) 'Mechanism of <scp>CaO</scp> catalyst deactivation with unconventional monitoring method for glycerol carbonate production via transesterification of glycerol with dimethyl carbonate, *International Journal of Energy Research*, 46(2), 1646–1658. Available at: https://doi.org/10.1002/er.7281 .
Ramola, B. and Joshi, N.C. (2019) 'Green Synthesis, Characterisations and Antimicrobial Activities of CaO Nanoparticles', *Oriental Journal of Chemistry,* 35(3), 1154–1157. Available at: https://doi.org/10.13005/ojc/350333 .
Rosdzimin, M.A., Rahim, A.M. and Author, C. (2020) Waste cooking oil biodiesel conversion using CaO of mussel shell as a heterogeneous catalyst, *Advances In Natural And Applied Sciences*, (2), 280–286. Available at: https://doi.org/10.22587/anas.2020.14.2.39 .
Rozina, Ahmad, M., Elnaggar, A.Y., Teong, L.K., Sultana, S., Zafar, M., Munir, M., Hussein, E.E. and Ul Abidin, S.Z. (2022) Sustainable and eco-friendly synthesis of biodiesel from novel and non-edible seed oil of Monotheca buxifolia using green nano-catalyst of calcium oxide, *Energy Conversion and Management*: X, 13, 100142. Available at: https://doi.org/10.1016/j.ecmx.2021.100142 .
Sahu, S., Saikia, K., Gurunathan, B., Dhakshinamoorthy, A. and Rokhum, S.L. (2023) 'Green synthesis of CaO nanocatalyst using watermelon peels for biodiesel production', *Molecular Catalysis*, 547(July), 113342. Available at: https://doi.org/10.1016/j.mcat.2023.113342
Seffati, K., Honarvar, B., Esmaeili, H. and Esfandiari, N.. (2019) 'Enhanced biodiesel production from chicken fat using CaO/CuFe2O4 nanocatalyst and its combination with diesel to improve fuel properties', *Fuel,* 235, 1238–1244. Available at: https://doi.org/10.1016/j.fuel.2018.08.118 .
Sivanesh, S., Aswin, K.N., Antony, A., Varma, M.S., Lekshmi, A., Kamalesh, K., Naageshwaran, M., Soundarya, S., and Subramanian, S. (2022) Biodiesel production from Custard apple seeds and Euglena Sanguinea using CaO nano-catalyst, *Bioresource Technology*, 344, 126418. Available at: https://doi.org/10.1016/j.biortech.2021.126418 .
Stani, C., Vaccari, L., Mitri, E. and Birarda, G. (2020) FTIR investigation of the secondary structure of type I collagen: New insight into the amide III band, *Spectrochimica Acta Part A: Molecular and Biomolecular Spectroscopy*, 229, 118006. Available at: https://doi.org/10.1016/j.saa.2019.118006 .
Sulaiman, S., Khairudin, S.N., Jamal, P. and Alam, M.Z. (2021) Fish Bone Waste as Catalyst for Biodiesel Production, *Journal of Tropical Resources and Sustainable Science (JTRSS),* 3(1), 180–184. Available at: https://doi.org/10.47253/jtrss.v3i1.554 .
Vinoth Arul Raj, J., Praveen Kumar, R., Vijayakumar, B., Gnansounou, E. and Bharathiraja, B. (2021) Modelling and process optimization for biodiesel production from Nannochloropsis salina using artificial neural network, *Bioresource Technology,* 329, 124872. Available at: https://doi.org/10.1016/j.biortech.2021.124872 .
Widayat, W., Darmawan,T., Hadiyanto, H., Ar-Rosyid, R. (2017) Preparation of Heterogeneous CaO Catalysts for Biodiesel Production. *J. Phys.: Conf. Ser.* 877 012018. https://doi.org/10.1088/1742-6596/877/1/012018
Zhang, J., Liu, J., Huang, X., Choi, S., Zhu, R., Tang, S., Bond, J.Q. and Tavlarides, L.L. (2020) Heterogeneous catalytic esterification of oleic acid under sub/supercritical methanol over γ-Al2O3, *Fuel,* 268(February), 117359. Available at: https://doi.org/10.1016/j.fuel.2020.117359 .